Structural Transition at Actin's N-Terminus in the Actomyosin Cross-Bridge Cycle†

James E. Hansen,‡ Joyce Marner,§ Dimitry Pavlov,|| Peter A. Rubenstein,§ and Emil Reisler*,‡

Department of Chemistry and Biochemistry and Molecular Biology Institute, University of California, Los Angeles, California 90095, Department of Biochemistry, College of Medicine, University of Iowa, Iowa City, Iowa 52242, and Department of Physiology, School of Medicine, University of California, Los Angeles, California 90095

Received August 10, 1999; Revised Manuscript Received November 4, 1999

ABSTRACT: Force and motion generation by actomyosin involves the cyclic formation and transition between weakly and strongly bound complexes of these proteins. Actin's N-terminus is believed to play a greater role in the formation of the weakly bound actomyosin states than in the formation of the strongly bound actomyosin states. It has been the goal of this project to determine whether the interaction of actin's N-terminus with myosin changes upon transition between these two states. To this end, a yeast actin mutant, Cys-1, was constructed by the insertion of a cysteine residue at actin's N-terminus and replacement of the C-terminal cysteine with alanine. The N-terminal cysteine was labeled stoichiometrically with pyrene maleimide, and the properties of the modified mutant actin were examined prior to spectroscopic measurements. Among these properties, actin polymerization, strong S1 binding, and the activation of S1 ATPase by pyrenyl-Cys-1 actin were not significantly different from those of wild-type yeast actin, while small changes were observed in the weak S1 binding and the in vitro motility of actin filaments. Fluorescence changes upon binding of S1 to pyrenyl-Cys-1 actin were measured for the strongly (with or without ADP) and weakly (with ATP and ATPγS) bound acto-S1 states. The fluorescence increased in each case, but the increase was greater (by about 75%) in the presence of MgATP and MgATPγS than in the rigor state. This demonstrates a transition at the S1 contact with actin's N-terminus between the weakly and strongly bound states, and implies either a closer proximity of the pyrene probe on Cys-1 to structural elements on S1 (most likely the loop of residues 626−647) or greater S1-induced changes at the N-terminus of actin in the weakly bound acto-S1 states.

Muscle contraction depends on dynamic interactions between actin and myosin coupled to ATP hydrolysis. During the cross-bridge cycle, the actomyosin complex cycles between strongly and weakly bound states. The strongly bound states correspond to actomyosin complexes AM·ADP (in the presence of ADP) and AM (in the absence of nucleotides), while the weakly bound states correspond to AM·ATP and AM·ADP·P_i complexes (in the presence of ATP and hydrolyzed ATP). The transition between these states is critical to the generation of force. The specific structural and mechanistic events that occur during the transition have not been determined, however, and a precise description of the actomyosin interface in both the strongly and weakly bound states remains a key goal in actomyosin research.

Actin's N-terminus has been identified for some time as being involved in the binding of S1.[1] Zero-length cross-linking reactions with carbodiimide couple actin's N-terminal acidic residues (*1*−*5*) to a group of basic residues on S1 within its loop 2, both in the presence and in the absence of ATP (*2*). On this basis, molecular models of the actomyosin interface predict that actin's acidic N-terminal residues interact with the lysine side chains in loop 2 (residues 626−647) on S1 (*4*−*6*). The importance of actin's acidic N-terminus is supported also by the fact that while actin isoforms differ in the number of acidic residues at the N-terminus, all have a net negative charge.

The results of immunochemical experiments confirmed the importance of actin's N-terminus, and suggested that it may play a greater role in the formation of the weakly bound states than in the formation of the strongly bound states. Antibodies that bind actin's N-terminus greatly reduce the level of weak acto-S1 binding, but have less effect on strong binding (*7*, *8*). Furthermore, blocking actin's N-terminus with these antibodies inhibits actin's ability to activate S1's ATPase (*6*) and to develop force in skinned muscle fibers (*9*). Taken together, the data from previous work clearly imply that actin's N-terminus has a significant and possibly dynamic role in the cross-bridge cycle.

In view of the suggested importance of actin's N-terminus, site-directed mutagenesis has been used to examine the functional consequences of changes in the sequence of the N-terminal residues. The substitution of histidine for acidic residues at the N-terminus in *Dictyostelium* actin inhibited

† This work was supported by United States Public Health Service Grant AR22031 and National Science Foundation Grant MCB9630997 (to E.R.) and National Institutes of Health Grant GM33689 (to P.A.R.).

‡ Department of Chemistry and Biochemistry and Molecular Biology Institute, University of California.

§ University of Iowa.

|| Department of Physiology, School of Medicine, University of California.

[1] Abbreviations: ATPγS, adenosine 5-(3-thio)triphosphate; BSA, bovine serum albumin; S1, myosin subfragment 1; DTT, dithiothreitol; HMM, heavy meromyosin; MOPS, 3-(*N*-morpholino)propanesulfonic acid; Tris, tris(hydroxymethyl)aminomethane.

10.1021/bi991873c CCC: $19.00
Published on Web 01/26/2000

filament sliding in the in vitro motility assays in the absence of methylcellulose and decreased the V_{max} of S1's actin-activated ATPase (*10*). In yeast actin, replacement of N-terminal residues aspartate and glutamate with asparagine and glutamine (DNEQ actin) yielded similar results (*11*, *12*). On the other hand, the addition of two negative charges to the N-terminus of yeast actin (4Ac actin) increased the V_{max} and catalytic efficiency of the actin-activated ATPase (*13*). The relative forces measured with the 4Ac actin in the in vitro motility assays in the presence of external load were almost 2-fold greater than those measured with the DNEQ actin (*12*). These studies provided further evidence that actin's N-terminus plays a significant part in the cross-bridge cycle but left open an important question. Does the interaction of the N-terminus of actin with S1 change during that cycle? Such a change and the involvement of the N-terminus of actin in the transition between the weakly and strongly bound states have been proposed in prior work (*14*−*16*).

This work takes advantage of a new yeast actin mutant, Cys-1, to address the above question and study the effect S1 binding has on actin's N-terminus in the strongly and weakly bound states. Cys-1 actin has an N-terminal cysteine residue which allows for the attachment of fluorescent probes (pyrene maleimide in this work). To ensure that only the N-terminal cysteine is labeled, Cys-1 actin has also had its Cys-374 replaced with alanine. Fluorescence measurements on the pyrene-labeled mutant actin at different concentrations of S1 allowed for monitoring the relative changes occurring at actin's N-terminus upon S1 binding. By comparing the fluorescence changes occurring at actin's N-terminus in the strongly and weakly bound states, we found that S1 binding induces greater changes at actin's N-terminus in the weakly bound states than in the strongly bound states. This provides direct evidence for a structural change at actin's N-terminus upon the transition from the weakly to the strongly bound actomyosin states, and confirms the role of actin's N-terminus in such a transition.

MATERIALS AND METHODS

Reagents. Yeast extract was purchased from Difco (Detroit, MI). Dextrose, DTT, and peptone were purchased from Fisher Scientific (Fair Lawn, NJ). ADP, ATP, β-mercaptoethanol, phalloidin, and phenylmethanesulfonyl fluoride were purchased from Sigma (St. Louis, MO). DNase I was obtained from Worthington Biochemical Corp. (Lakewood, NJ). ATPγS was purchased from Boehringer Mannheim (Mannheim, Germany). Rhodamine phalloidin and pyrene maleimide were from Molecular Probes (Eugene, OR), and the Bio-Rad protein assay and Affigel-10 were purchased from Bio-Rad Laboratories (Hercules, CA).

Construction of the $M_1CD_2/C_{374}A$ (MCDCA) Actin Mutant. The construction of a double actin mutation Cys-1, in which a cysteine codon is inserted between the initiator methionine and the following aspartate and the Cys-374 residue is converted to Ala, was started with pCENMCD (*11*), a URA3-marked YCp50 derivative containing the yeast actin coding sequence with the M_1CD_2 mutation adjacent to the yeast actin promoter. The 1.8 kb *Eco*RI−*Hin*dIII fragment containing the $C_{374}A$ mutation was excised from plasmid pGEMCA (*17*) and substituted for the homologous fragment in pCENMCD to create pCENMCDCA. This plasmid was used to transform a haploid yeast strain derived from TDyDD with a deleted chromosomal actin gene that contained a wild-type actin gene in the TRP1 marked plasmid pRS314 (*18*). Transformants were then selected for growth in ura$^-$ medium, and subsequent selection for growth on trp$^+$, ura$^-$ medium produced cells containing only the pCENMCDCA plasmid. Sequencing of the entire actin coding sequence of the plasmid re-isolated from the yeast demonstrated that the plasmid contained only the two desired mutations. The cells exhibited a normal morphology and grew at normal rates in complete medium (YPD) at 30 °C.

Preparation of Proteins. Yeast actin was purified by a modification of the DNase I procedure of Cook et al. (*19*). Actin was eluted from the DNase I column with 50% formamide in G-buffer [10 mM Tris, 0.2 mM $CaCl_2$, and 2.0 mM β-mercaptoethanol (pH 7.8)] directly onto a 1 mL DE52 DEAE-cellulose column equilibrated in G-buffer. Following a G-buffer wash, the actin was eluted with G-buffer containing 0.3 M KCl. After dialysis against G-buffer, the actin was put through a polymerization/depolymerization cycle, and the final G-actin preparation was stored at 4 °C and used within 1 week. Yields (approximately 1 mg of actin from 100 g of cells) were approximately $^1/_3$ to $^1/_4$ of that achieved with wild-type actin, as is usually the case when actin contains the C374A mutation. Wild-type yeast actin retains the initiator methionine since the second amino acid, Asp, prevents cleavage by the methionine aminopeptidase. However, this enzyme will remove methionine when the second amino acid is Cys. Previous work with MCD actin showed that the initiator methionine was removed and 70% of the protein began with *N*-acetylcysteine while the remainder began with free cysteine (*11*). The same should be true with MCDCA actin since the residue at 374 has no bearing on the activity of the methionine aminopeptidase. Therefore, we refer to the inserted cysteine as Cys-1. Actin concentrations were determined using the Bradford assay (*20*).

Myosin was prepared by the method of Godfrey and Harrington (*21*), and S1 was prepared from this myosin by chymotryptic digestion according to the procedure of Weeds and Pope (*22*).

Binding Measurements. Acto-S1 binding in the presence and absence of nucleotides was assessed by cosedimentation experiments. For strong binding measurements, 4.0 μM G-actin (free of unbound ATP) was prepolymerized with 3.0 mM $MgCl_2$ and 4.0 μM phalloidin. S1 was prespun prior to mixing with actin to remove any aggregated protein. Actin was then incubated with S1 at concentrations ranging between 0 and 10 μM in 100 mM KCl and 10 mM imidazole at pH 7.4 and 22 °C in the absence and presence of 3.0 mM MgADP. Samples of these mixtures were pelleted for 10 min at 140000*g* in a Beckman airfuge. The supernatants were removed; the pellets were resuspended in fresh buffer, and both were subjected to SDS−PAGE analysis on a 10% gel (*23*). The molar ratio of S1 bound to actin was determined by the density of the resulting bands using Sigmagel and calibrations of S1 and actin staining. K_d values were determined by fitting the data to the curve described by the binding equation

$$S_{bound}/A = \{(A + S + K_d) - [(A + S + K_d)^2 - 4AS]^{1/2}\}/2A \quad (1)$$

where A and S represent total actin and S1 concentrations, respectively, S_{bound} represents the concentration of S1 bound to actin, and K_d corresponds to the dissociation constant of the acto-S1 complex. The equation assumes 1:1 binding of S1 to actin.

Measurements of weak binding of S1 to actin in the presence of 3.0 mM MgATP, 5.0 mM ATPγS, and 10 mM MgATPγS followed the procedure described above except that higher concentrations of S1 had to be used to detect binding, and the solvent contained 10 mM KCl and 10 mM imidazole at pH 7.4 and 22 °C.

Actin-Activated S1 ATPase Assays. Actin was prepolymerized by 3.0 mM $MgCl_2$ and an equimolar amount of phalloidin, and incubated with 0.5 μM S1. ATP (1.0 mM) was added to the mixtures to begin the reaction, which was then stopped with the addition of equal volumes of 0.6 M perchloric acid. Precipitated proteins were removed by centrifugation. The amount of released phosphate in the supernatant was determined by the Malachite Green Assay according to the method of Kodama et al. (*24*). Because the preparation of Cys-1 actin yields small amounts of protein, it was difficult to reach concentrations of actin that are high enough to determine the K_m and V_{max} values. Therefore, we compared the activation of S1's ATPase by pyrenyl-Cys-1 actin to the activation by wild-type actin at three concentrations of actin (5.0, 10, and 15 μM).

Labeling of Cys-1 Actin with Pyrene Maleimide. Before labeling, Cys-1 actin was dialyzed overnight against G-actin buffer lacking β-mercaptoethanol. After dialysis, Cys-1 actin was polymerized with 3.0 mM $MgCl_2$, and pyrene maleimide equimolar to the actin concentration was added at the same time. The mixture was allowed to react for 90 min at room temperature, and then in a cold box overnight. The reaction mixture was then spun in a Beckman ultracentrifuge for 3 h at 226000*g* to pellet out the polymerized, labeled actin. The labeling stoichiometry was determined by absorption measurements, and was typically between 0.9 and 1.1 pyrene/Cys-1 actin.

Fluorescence Measurements and Fluorescence Titrations of Actin with S1. Fluorescence measurements were carried out using a Spex Fluorolog spectrofluorometer (Spex Industries, Edison, NJ) at 25 °C. For pyrenyl-Cys-1 actin fluorescence, the excitation wavelength used for emission scans and for time-based scans was 339 nm, and the emission wavelength used for excitation and time-based scans was 373 nm.

For titrations of pyrenyl-Cys-1 actin with S1 in the presence and absence of ADP, the actin was polymerized with 3.0 mM $MgCl_2$ and an equimolar amount of phalloidin, and then diluted to 4.0 μM in G-actin buffer lacking ATP. When present, MgADP (3.0 mM) was added to the cuvette. The emission of the pyrenyl-Cys-1 actin was recorded at the emission maximum as successive aliquots of S1 were added to the same cuvette. These fluorescence data were corrected for the dilution caused by the addition of S1.

Titrations with S1 in the presence of ATP and ATPγS were performed in the same way as described above, except that 3.0 mM MgATP and 5.0 or 10 mM MgATPγS were added to the cuvette, higher concentrations of S1 were used, and separate cuvettes were used for each concentration of S1 to avoid excessive hydrolysis of ATP.

In Vitro Motility Assay. Heavy meromyosin (HMM) preparation followed the protocol of Kron et al. (*25*). To eliminate HMM heads that are desensitized to ATP, the HMM was centrifuged with actin in a solution containing 50 mM KCl, 25 mM MOPS, 1.0 mM EGTA, 4.0 mM $MgCl_2$, and 3.0 mM MgATP (pH 7.4) for 30 min in a Beckman airfuge. The supernatant HMM was then applied to nitrocellulose-treated cover slips at a concentration of 0.2−0.3 mg/mL. The remaining surface of the cover slip was coated with BSA. The excess of proteins was washed off with assay buffer [25 mM KCl, 1.0 mM EGTA, 4.0 mM $MgCl_2$, 10 mM dithiothreitol, and 25 mM MOPS (pH 7.4)]. Actin filaments were incubated overnight with an equimolar concentration of rhodamine phalloidin, and were then pelletted by centrifuging for 45 min in a Beckman airfuge. The labeled filaments were then resuspended in buffer and added to the coated cover slips at a concentration of 10 nM. Filaments that did not bind to the HMM were washed away with the assay buffer. For high-salt assay solutions, the ionic strength was increased to 100 mM by the addition of KCl. The motion of the filaments remaining on the cover slip was initiated by the addition of a motility solution, composed of assay buffer containing 25 mM KCl (or more), 1.0 mM ATP, and, acting as an oxygen scavenging system, glucose (3.0 mg/mL), glucose oxidase (24 units/mL), and catalase (0.2 mg/mL). The temperature was maintained at 25 °C for all assays. The movement of the filaments was recorded and analyzed for sliding speeds using an Expertvision system (Motion Analysis, Santa Rosa, CA). For statistical analysis, only those filaments with standard deviations of less than $^1/_2$ of the average velocity were used.

Electron Microscopy. Wild-type and pyrenyl-Cys-1 actin were polymerized by 3.0 mM $MgCl_2$ and phalloidin equimolar to the actin concentration, and were mounted for electron microscopy as described by Kim et al. (*26*). Micrographs of the actin filaments were taken at an apparent magnification of 30000×.

RESULTS

Functional Properties of Labeled Cys-1 Yeast Actin. Cys-1 actin, the mutant used in this project, was constructed by placing a cysteine residue at actin's N-terminus, along with replacing its C-terminal cysteine with an alanine. This mutant opened up the possibility of introducing a fluorescent probe at the N-terminus of actin and characterizing, via such a probe, the changes that occur at this part of actin when S1 interacts with the mutant protein. However, any interpretation of spectroscopic data required a prior evaluation of functional properties of the mutant actin.

Motion of Cys-1 Actin in the in Vitro Motility Assays. The in vitro motility assay directly tests the overall actin function in the cross-bridge cycle. Measurements of the sliding of pyrenyl-Cys-1 actin filaments over heavy meromyosin in low salt in the presence and absence of methylcellulose, and in high salt in the presence of methylcellulose, allowed such an overall assessment of pyrenyl-Cys-1 actin function. Methylcellulose, a viscosity-enhancing agent, hinders diffusion of the actin filaments away from the HMM, and this prevents or inhibits motility loss in those cases in which the weak actomyosin interactions are inhibited. Under low-salt conditions (50 mM ionic strength), pyrenyl-Cys-1 actin

Table 1: Motion of Pyrenyl-Cys-1 Actin Filaments in the in Vitro Motility Assays[a]

assay conditions	wild-type filaments (μm/s)	pyrenyl-Cys-1 filaments (μm/s)
low salt (I = 50 mM) (without methylcellulose)	3.40 ± 0.2	3.10 ± 0.1
low salt (50 mM) (with methylcellulose)	3.50 ± 0.1	3.30 ± 0.2
high salt (100 mM) (with methylcellulose)	3.40 ± 0.1	3.60 ± 0.2

[a] Speeds of wild-type and pyrenyl-Cys-1 actin filaments were measured in the in vitro motility assays at 25 °C under three different conditions: low salt (50 mM ionic strength) in the absence of methylcellulose, low salt in the presence of methylcellulose, and high salt (100 mM ionic strength) in the presence of methylcellulose. Mean speeds of smoothly moving filaments are reported with standard errors of the means. The motion of 150−250 filaments was measured in each experiment.

filaments moved at a mean speed of 3.10 ± 0.1 μm/s, while the wild-type actin filaments moved slightly faster, at a mean speed of 3.40 ± 0.2 μm/s (Table 1). As expected, the addition of methylcellulose to the medium did not significantly improve the sliding speeds (3.50 ± 0.1 μm/s) of the wild-type actin filaments. Similarly, methylcellulose addition did not significantly change the sliding speeds (3.30 ± 0.2 μm/s) of the pyrenyl-Cys-1 actin filaments (Table 1). Under high-salt conditions and in the presence of methylcellulose, the wild-type and pyrenyl-Cys-1 actin filaments moved at similar speeds, 3.40 ± 0.1 and 3.60 ± 0.2 μm/s, respectively (Table 1). Because methylcellulose (under low-salt conditions) and high ionic strength do not affect the sliding speeds of pyrenyl-Cys-1 actin filaments, the mutation and modification of actin's N-terminus must not have greatly inhibited the weak interactions between the actin filaments and the HMM heads. However, some decrease in the level of acto-S1 binding is indicated by the fact that under all conditions the percentage of actin filaments moving smoothly over HMM was between 20 and 25% smaller for the labeled mutant than for wild-type actin. Sparrow and his group have studied a similar mutant which retains an *N*-acetylated Cys-1 in actin from *Drosophila* flight muscles (Act88F). For reasons unclear to us, the in vitro motility of their mutant actin was impacted much more than that of pyrenyl-Cys-1 actin by the absence of methylcellulose in these assays (Sparrow, personal communication).

Polymerization of Cys-1 Actin and Filament Structure. The rate of polymerization of Cys-1 actin by $MgCl_2$, as measured by monitoring increases in light scattering, did not differ significantly from that of wild-type actin (data not shown). A comparison of the fluorescence of actin monomer (G-actin) and polymer (F-actin), i.e., the emission and excitation spectra recorded for 4.0 μM pyrenyl-Cys-1 actin before (G-actin) and after the addition of 3.0 mM $MgCl_2$ and 4.0 μM phalloidin (F-actin), revealed no differences between the two forms of actin. This demonstrates that polymerization of Cys-1 actin has no effect on the environment of the pyrene probe on actin (Figure 1). This is consistent with models of F-actin structure in which the N-terminus of actin is distant from the polymerization interface (*5*, *27*) and the fact that the antibodies to the N-terminus do not alter the kinetics of actin polymerization (*28*). Visual inspection of electron micrographs of phalloidin-stabilized wild-type and pyrenyl-Cys-1 actin did not reveal any morphological difference between the two polymers except for a minor increase in the fraction of short filaments in the mutant case.

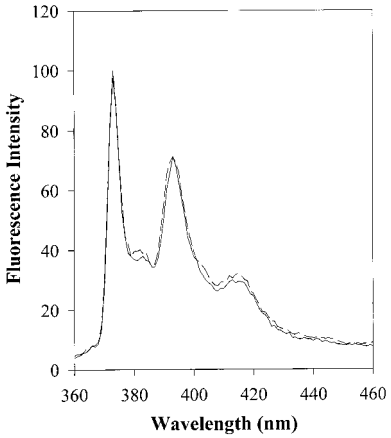

FIGURE 1: Emission spectra of pyrenyl-Cys-1 G-actin and F-actin. Emission spectra of 4.0 μM pyrenyl-Cys-1 actin (λ_{ex} = 339 nm) were recorded before polymerization, shown as a solid curve (G-actin), and after the polymerization, shown as a dashed curve (F-actin). Polymerization of G-actin to F-actin was induced by the addition of 3.0 mM $MgCl_2$ and 4.0 μM phalloidin.

Binding of S1 to Cys-1 Yeast Actin. The binding of pyrenyl-Cys-1 actin to S1 was assessed by cosedimentation assays under strong (in the presence of ADP and in the absence of nucleotide) and weak binding conditions (in the presence of ATP and ATPγS). K_d values obtained from such measurements were used then to correlate the observed changes in pyrenyl-Cys-1 actin fluorescence with the amount of S1 bound to actin. For rigor binding, S1 concentrations ranged between 0 and 10 μM, and the data were fitted to an equation describing single-site binding of S1 to actin (eq 1). Wild-type actin and pyrenyl-Cys-1 mutant actin bound S1 equally well, and their binding data were described by the same curve, with a K_d of 2.0 ± 0.2 μM (Figure 2). Similar binding measurements carried out with pyrenyl-Cys-1 actin in the presence of 3.0 mM MgADP yielded a K_d of 5.5 ± 1.5 μM (Table 2).

Measurements of weak binding of S1 to actin followed the same procedure as described above, except that concentrations of S1 ranged between 0 and 40 μM in the presence of 3.0 mM MgATP or 5.0 mM MgATPγS, and up to 60 μM in the presence of 10 mM MgATPγS. Under the weak binding conditions, the pyrenyl-Cys-1 mutant actin had approximately 2-fold lower affinity for S1 than the wild-type actin. In the presence of 3.0 mM MgATP, the K_d values describing the binding of S1 to wild-type and pyrenyl-Cys-1 actin were 14 ± 1.5 and 26 ± 1.3 μM, respectively (Figure 3). To analyze fluorescence measurements in the presence of MgATPγS, a binding curve was also obtained for pyrenyl-Cys-1 actin in the presence of 10 mM MgATPγS, with a K_d of 66 ± 2 μM (Figure 3). The higher K_d value in this case is due to the increased ionic strength of the solution containing 10 mM ATPγS. Overall, the binding data demonstrated that the labeled mutant actin filaments bind S1 with an approximately 2-fold lower affinity than wild-type actin in the presence of ATP, but showed no difference in rigor binding affinity.

Another important test of the function of a new actin mutant is its ability to activate the ATPase activity of S1.

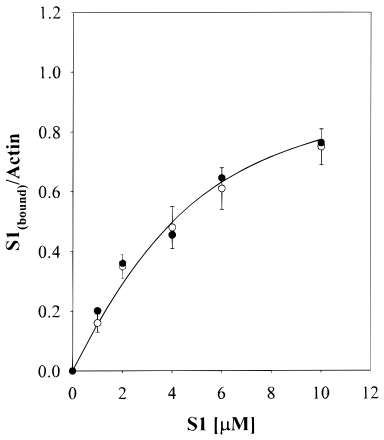

FIGURE 2: Strong S1 binding of wild-type and pyrenyl-Cys-1 actin. The strong binding of both wild-type and pyrenyl-Cys-1 actin to S1 was assessed in cosedimentation assays. Actin (4.0 μM) was prepolymerized by 3.0 mM $MgCl_2$ and 4.0 μM phalloidin, and incubated with S1 at concentrations ranging between 0 and 10 μM in 100 mM KCl and 10 mM imidazole at pH 7.4 and 22 °C. Samples were pelleted for 10 min at 140000*g* in a Beckman airfuge, and the pellets were resuspended, denatured, and subjected to SDS−PAGE analysis. The binding data for wild-type actin (●) and pyrenyl-Cys-1 actin (○) fit the same curve, described by a K_d of 2.0 ± 0.2 μM. The data for wild-type actin are the mean values of three independent binding experiments, and those for the mutant actin are the mean of eight sets of experiments. Standard deviations are represented by the bars.

Table 2: Summary of K_d Values for S1 Binding to Pyrenyl-Cys-1 Actin[a]

nucleotide	binding state represented	K_d (μM)
−	AM	2.0 ± 0.2
3.0 mM MgADP	AM·ADP	5.5 ± 1.5
3.0 mM MgATP	AM·ADP·P_i	26 ± 1.3
5.0 mM MgATPγS	AM·ATP	39 ± 6.0
10 mM MgATPγS	AM·ATP	66 ± 2.0

[a] The K_d values for the binding of S1 to pyrenyl-Cys-1 actin in the presence of each nucleotide are listed, along with the represented state in the kinetic scheme of the cross-bridge cycle. The binding of S1 to actin was assessed in cosedimentation assays in buffers containing either 10 mM (in the presence of ATP and ATPγS) or 100 mM KCl (in the presence and absence of ADP). The K_d values were obtained from plots shown in Figures 2 and 3 or from similar plots.

At three actin concentrations (5.0, 10, and 15 μM), pyrenyl-Cys-1 actin activated S1's ATPase to nearly the same degree as wild-type actin. Determinations of K_m and V_{max} values of acto-S1 ATPase were not attempted because of limited amounts of the mutant actin. Together with the motility and S1 binding results, this suggests that the modification of actin's N-terminus does not alter significantly any of the actomyosin interaction parameters and actin's function.

Fluorescence Probing of the Acto-S1 Interactions at Actin's N-Terminus. (1) Strong Binding Titration. To determine the effect of S1 on pyrenyl-Cys-1 actin fluorescence, emission scans of 4.0 μM pyrenyl-Cys-1 actin in the presence and absence of 10 μM S1 were compared. In the presence of 10 μM S1, pyrenyl-Cys-1 actin's fluorescence increased approximately 60% (Figure 4). The fluorescence of pyrenyl-Cys-1 actin was then monitored at the emission maximum (373 nm) at increasing concentrations (0−20 μM) of S1 under rigor conditions. The fluorescence increases followed a clear binding saturation curve, reaching a calculated maximum of an 83% increase over the baseline fluorescence.

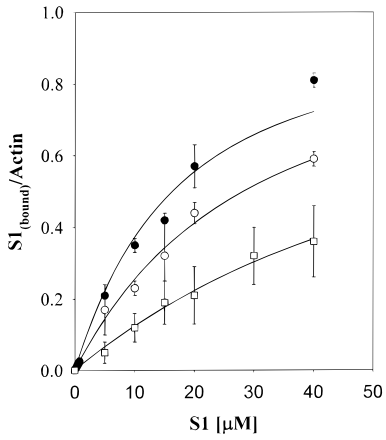

FIGURE 3: Weak acto-S1 binding of wild-type and pyrenyl-Cys-1 actin. The weak binding of both wild type and pyrenyl-Cys-1 actin to S1 was assessed in cosedimentation assays. Actin (4.0 μM) was prepolymerized by 3.0 mM $MgCl_2$ and 4.0 μM phalloidin, and incubated with S1 at concentrations ranging between 0 and 40 μM in 10 mM KCl and 10 mM imidazole at pH 7.4 and 22 °C. MgATP (3.0 mM) and ATPγS (10 mM) were added to these mixtures prior to centrifugation. Samples were pelleted at 140000*g* in a Beckman airfuge, and the pellets were resuspended, denatured, and subjected to SDS−PAGE analysis. All binding data were fitted to eq 1 (Materials and Methods). The binding data for the wild-type actin in the presence of 3.0 mM MgATP (●) yielded a K_d of 14 ± 1.5 μM. Pyrenyl-Cys-1 actin bound to S1 in the presence of 3.0 mM MgATP (○) with a K_d of 26 ± 1.3 μM, and with a K_d of 66 ± 2 μM in the presence of 10 mM MgATPγS (□). The data are the mean values of four independent binding experiments. Standard deviations are represented by the bars.

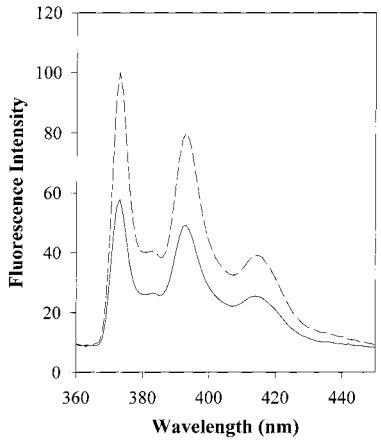

FIGURE 4: Emission spectra of pyrenyl-Cys-1 actin in the presence and absence of S1. Pyrenyl-Cys-1 actin was prepolymerized by 3.0 mM $MgCl_2$ in the presence of an equimolar amount of phalloidin, and then diluted to 4.0 μM in G-actin buffer containing $MgCl_2$ but lacking ATP, such that the final concentration of ATP in the cuvette was approximately 40 μM. Emission spectra were taken prior to (solid curve) and after the addition of 10 μM S1 (dashed curve). λ_{ex} = 339 nm.

Fitting the data to a binding curve yields a K_d of 2.1 ± 0.6 μM (Figure 5), which closely matches the K_d calculated for pyrenyl-Cys-1 actin rigor binding of S1 in cosedimentation assays. The close correlation between the two K_d values validates the conclusion that it is S1 binding that causes the fluorescence increase, and, in turn, the fluorescence increase indicates an interaction between S1 and actin's N-terminus under rigor conditions. Similar fluorescence titrations were carried out also for the binding of S1 to pyrenyl-Cys-1 actin in the presence of 3.0 mM MgADP. The results of these

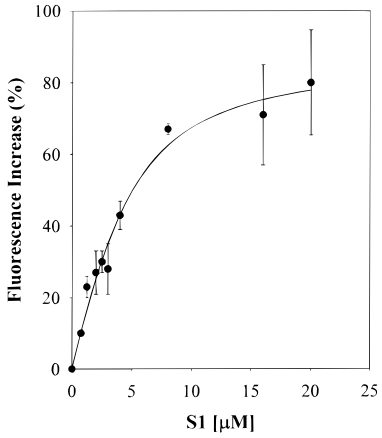

FIGURE 5: Effect of S1 on the fluorescence of pyrenyl-Cys-1 actin in the absence of nucleotides. Pyrenyl-Cys-1 actin was prepolymerized with 3.0 mM $MgCl_2$ in the presence of an equimolar amount of phalloidin and diluted to a final concentration of 4.0 μM in G-actin buffer containing $MgCl_2$ but lacking ATP such that the final concentration of ATP in the cuvette was approximately 40 μM. Pyrenyl-Cys-1 actin was then excited at 339 nm, and its fluorescence was measured at the emission maximum (373 nm) as successive aliquots of S1 were added. The increases in fluorescence were recorded and corrected for dilution. The percentage increases in fluorescence were plotted against the concentration of S1 added, and the data yielded a K_d of 2.1 $\pm$ 0.6 μM. The data are the mean of six independent experiments. Standard deviations are represented by the bars.

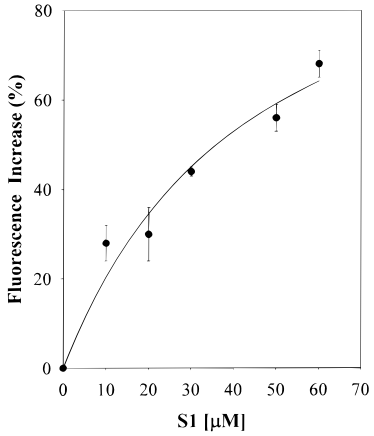

FIGURE 6: Effect of S1 on the fluorescence of pyrenyl-Cys-1 actin in the presence of 10 mM ATPγS. Titrations with S1 in the presence of 10 mM ATPγS were carried out in the same way as in the absence of ATP, except that higher concentrations of S1 were used (up to 60 μM), and 10 mM ATPγS was added to the cuvette. The data were again plotted against the concentration of S1 that was added, and yielded a K_d of 40.2 $\pm$ 19.3 μM. The same titrations were also carried out in the presence of 3.0 mM MgATP and 5.0 mM MgATPγS (λ_{ex} = 339 nm, λ_{em} = 373 nm). The data are the mean values of three independent experiments. Standard deviations are represented by the bars.

titrations are presented in the final plot correlating fluorescence increases with the level of S1 binding to actin (Figure 7).

(2) Weak Binding Titrations. To measure the effect S1 has on pyrenyl-Cys-1 actin fluorescence under weak binding conditions, the fluorescence titrations were performed in the presence of MgATPγS (5.0 and 10 mM) and MgATP (3.0 mM). ATPγS, a slowly hydrolyzed analogue of ATP, allowed the use of higher concentrations of S1, and thus, higher ratios of S1 bound to actin could be reached without the complication of nucleotide hydrolysis. The weakly bound

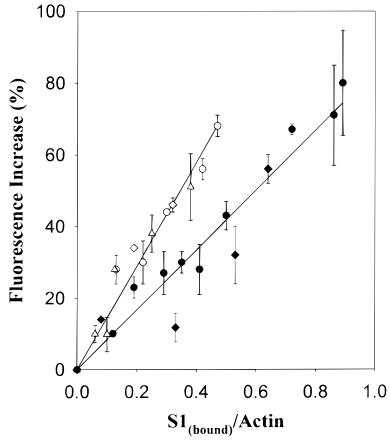

FIGURE 7: Comparison of the effects of S1 on the fluorescence of pyrenyl-Cys-1 actin in the weakly and strongly bound states. The percentage increase in pyrenyl-Cys-1 actin fluorescence was plotted against the fraction of S1 bound to actin, which was calculated from the K_d values listed in Table 2. Linear plots describe the effect of S1 on pyrenyl-Cys-1 actin fluorescence in both the weak binding states (3.0 mM MgATP, 5.0 mM MgATPγS, and 10 mM MgATPγS) and the strong binding states (no nucleotide or 3.0 mM MgADP). The slope of the line fitting to the weak binding states is approximately 75% greater than the slope of the line fitting to the strong binding states: (●) no nucleotide, (◆) 3.0 mM MgADP, (○) 10 mM MgATPγS, (◇) 5.0 mM MgATPγS, and (△) 3.0 mM MgATP.

state which is probed under such conditions is an analogue of the AM·ATP state. A plot of the increases in pyrenyl-Cys-1 actin fluorescence versus S1 concentration in the presence of 10 mM MgATPγS yields a curve with a K_d of 40.2 $\pm$ 19.3 μM (Figure 6). This K_d matches well the K_d determined for pyrenyl-Cys-1 actin binding to S1 in the presence of 10 mM ATPγS (66 $\pm$ 2 μM), which demonstrates that the interaction between S1 and actin's N-terminus causes the fluorescence increase. Similar plots were generated by titrations of pyrenyl-Cys-1 actin with S1 in the presence of 5.0 mM Mg-ATPγS and 3.0 mM Mg-ATP and were converted to the final representation of fluorescence versus fraction of actin bound to S1 (Figure 7). In the case of MgATP, the AM·ADP·P_i complex represents the dominant species present in the solution. Thus, the use of ATPγS and ATP allows for probing the environment of actin's N-terminus in the two types of weakly bound states, AM·ATP and AM·ADP·P_i.

Comparison of the Effect of S1 on Pyrenyl-Cys-1 Actin Fluorescence in Weak versus Strong Binding States. Given the conclusion that S1 binding causes an increase in pyrenyl-Cys-1 actin fluorescence, and assuming the absence of cooperative changes in actin filaments due to S1 binding, one might expect to observe a linear dependence of pyrene fluorescence on the amount of S1 bound to actin. Plotting the percentage increase in pyrenyl-Cys-1 actin's fluorescence versus the fraction of S1 bound to actin (calculated using the K_d values obtained from the binding experiments, Table 2) indeed yields such a result (Figure 7). Linear plots were obtained for S1-induced increases in pyrenyl-Cys-1 actin fluorescence with an increased level of S1 binding for both the strongly and weakly bound acto-S1 complexes. A single straight line can describe the fluorescence changes for the strong S1 binding to actin in the presence and absence of MgADP. Similarly, a single straight line can describe the fluorescence changes for the weak S1 binding to actin in

the presence of 3.0 mM MgATP, 5.0 mM MgATPγS, or 10 mM MgATPγS. The slope of the line describing the fluorescence changes occurring in the weak binding states is about 75% greater than the slope of the line describing the fluorescence changes in the strong binding states. Thus, at 50% saturation of actin by S1, the fluorescence increase is about 40 and 70% in the strongly and weakly bound states, respectively (Figure 7).

DISCUSSION

The goal of this study was to determine using labeled Cys-1 mutant yeast actin whether the interaction of actin's N-terminus with myosin changes upon transition from weakly to strongly bound actomyosin states. Naturally, the use of a modified, mutant actin to probe transitions at the actomyosin interface required prior functional evaluation of the new actin. Overall, the results of such evaluation, including the binding experiments, electron microscopy observations, ATPase experiments, and in vitro motility assays, validate the use of the mutant in studies of the interaction between S1 and actin at actin's N-terminus. Neither the mutation nor the pyrenyl probe significantly alters the main parameters of actomyosin interactions and function. Accordingly, the effect of S1 on the fluorescence of pyrenyl-Cys-1 mutant actin was determined in both the strong and weak acto-S1 binding states.

Acto-S1 Interactions and the N-Terminus of Actin. To compare the relative effect of S1 on pyrenyl-Cys-1 actin fluorescence in the strongly and weakly bound states, fluorescence titrations were carried out in both states. In both cases, the fluorescence data yielded K_d values similar to those determined in the cosedimentation assays. This correlation supports the conclusion that the observed increases in pyrenyl-Cys-1 actin fluorescence are in fact due to S1 binding.

To directly compare the changes in fluorescence seen in the strong and weak binding states, the percentage increase in fluorescence for both states was plotted against the fraction of S1 bound to pyrenyl-Cys-1 actin, as calculated from K_d values listed in Table 2. In the absence of nucleotides, in the AM state of the cross-bridge cycle, S1 binding increased the fluorescence of pyrenyl-Cys-1 actin by close to 75% (at binding saturation), demonstrating a significant change in the probe's environment. The effect of S1·ADP on pyrenyl-Cys-1 actin's fluorescence (in the presence of 3.0 mM MgADP), i.e., in the AM·ADP state of the cross-bridge cycle, was indistinguishable from that of S1 alone (Figure 7). A single line describes the fluorescence change in the strong binding (AM and AM·ADP) states, indicating that the interaction between S1 and actin's N-terminus is independent of the presence of ADP. Similarly, a single line describes the fluorescence changes in the weak binding states. The data from the titrations in the presence of MgATP may be taken as representative of the AM·ADP·P_i state, and the data from the titrations in the presence of ATPγS may be taken as representative of the AM·ATP state. Since a single line fits both sets of data, it appears that the fluorescence change in the weak binding states is independent of the hydrolysis state of the nucleotide. Furthermore, the fluorescence change in the weak binding states is independent of the small difference in ionic strength and the K_d value for S1 binding to actin (between 3.0 mM MgATP and 10 mM MgATPγS). A comparison of the fluorescence changes in the strong and weak binding states shows that the slope of the fluorescence increase line is greater (by about 75%) for the weakly bound than for the strongly bound acto-S1 states (Figure 7). This result provides clear evidence of a change in the environment of actin's N-terminus upon transition between the weakly bound and the strongly bound states in the cross-bridge cycle.

The greater change in pyrene fluorescence observed in the weakly bound states suggests an "increased interaction" between S1 and actin's N-terminus in such states. Several possible explanations for such an increased interaction come to mind. The N-terminus of actin and the pyrene probe may be in closer contact or proximity to structural elements on S1 (probably the loop of residues 626−647) in the weakly bound states. The conformation of loop 2 on S1 is probably different and most likely more structured in the strongly bound acto-S1 states (*14*, *15*), and the N-terminus of actin may interact with different residues of this loop in the two states. Such a change would lead to a different microenvironment and fluorescence of the Cys-1 probe in the strongly and weakly bound states. In principle, even bigger changes in the S1 binding site for the N-terminus of actin, including a possible interaction with a structural element different from loop 2, could be contemplated. In such a scenario, the N-terminus of actin would bind to loop 2 in the weakly bound states, as suggested by prior biochemical and immunochemical studies, and could switch to a different location on S1 in the rigor complexes. However, more extensive remodeling of acto-S1 contacts upon its transition to the strongly bound state is contradicted by carbodiimide cross-linking of the N-terminus of actin to loop 2 in rigor acto-S1 complexes (*3*). Obviously, even small changes in the S1 binding site for actin's N-terminus may involve structural changes in that part of actin, resulting in the observed differences in pyrenyl-Cys-1 fluorescence in the weakly and strongly bound acto-S1 states. Future experiments using energy transfer between a probe on Cys-1 and a label located elsewhere on Cys-1 actin (such as fluorescein phalloidin) may help in resolving some of these explanations by providing information about possible changes in the location of actin's N-terminus relative to other parts of actin during the cross-bridge cycle. The main importance of this work is in providing the experimental evidence for a change in a specific acto-S1 contact, involving the N-terminus of actin, upon transition between weakly and strongly bound states.

ACKNOWLEDGMENT

We thank Dr. Earl Homsher for his help during the project. We also thank Dr. Martin Phillips for taking the electron micrographs of actin filaments and Elena Bobkova for help with the in vitro motility measurements.

REFERENCES

1. Mornet, D., Bertrand, R., Pantel, P., Audemard, E., and Kassab, R. (1981) *Nature 292*, 301−306.
2. Yamamoto, K. (1989) *Biochemistry 28*, 5573−5577.
3. Sutoh, K. (1982) *Biochemistry 21*, 3654−3661.
4. Schröder, R. R., Manstein, D. J., Jahn, W., Holden, H., Rayment, I., Holmes, K. C., and Spudich, J. A. (1993) *Nature 364*, 171−174.

5. Holmes, K. C., Popp, D., Gebhard, W., and Kabsch, W. (1990) *Nature 347*, 44−49.
6. Rayment, I., Holden, H. M., Whittaker, M., Yohn, C. B., Lorenz, M., Holmes, K. C., and Milligan, R. A. (1993) *Science 261*, 58−65.
7. DasGupta, G., and Reisler, E. (1989) *J. Mol. Biol. 207*, 833−836.
8. DasGupta, G., and Reisler, E. (1991) *Biochemistry 30*, 9961−9966.
9. Brenner, B., Kraft, T., DasGupta, G., and Reisler, E. (1996) *Biophys. J. 70*, 48−56.
10. Sutoh, K., Ando, M., and Toyoshima, Y. Y. (1991) *Proc. Natl. Acad. Sci. U.S.A. 74*, 5463−5467.
11. Cook, R. K., Sheff, D. R., and Rubenstein, P. A. (1991) *J. Biol. Chem. 266*, 16825−16833.
12. Miller, C. J., Wong W. W., Bobkova, E., Rubenstein, P. A., and Reisler, E. (1996) *Biochemistry 35*, 16557−16565.
13. Cook, R. K., Root, D., Miller, C., Reisler, E., and Rubenstein, P. A. (1993) *J. Biol. Chem. 268*, 2410−2415.
14. Holmes, K. C. (1995) *Biophys. J. 68*, 2s−7s.
15. Miller, C. J., Cheung, P., White, P., and Reisler, E. (1995) *Biophys. J. 68*, 50s−54s.
16. Kim, E., Miller, C. J., and Reisler, E. (1996) *Biochemistry 35*, 16566−16572.
17. Feng, L., Kim, E., Lee, W. L., Miller, C. J., Kuang, B., Reisler, E., and Rubenstein, P. A. (1997) *J. Biol. Chem. 272*, 16829−16837.
18. Chen, X., and Rubenstein, P. A. (1995) *J. Biol. Chem. 270*, 11406−11414.
19. Cook, R. K., Root, D., Miller, C. J., Reisler, E., and Rubenstein, P. A. (1993) *J. Biol. Chem. 268*, 2410−2415.
20. Bradford, M. M. (1976) *Anal. Biochem. 72*, 248−254.
21. Godfrey, J. E., and Harrington, W. F. (1970) *Biochemistry 9*, 886−895.
22. Weeds, A., and Pope, A. B. (1977) *J. Mol. Biol. 111*, 129−157.
23. Laemmli, U. K. (1970) *Nature 227*, 680−685.
24. Kodama, T., Fukui, K., and Kometani, K. (1986) *J. Biochem. 99*, 1465−1472.
25. Kron, S. J., Toyoshima, Y. Y., Uyeda, T. Q., and Spudich, J. A. (1991*) Methods Enzymol. 196*, 399−416.
26. Kim, E., Phillips, M., Hegyi, G., Muhlrad, A., and Reisler, E. (1998) *Biochemistry 37*, 17793−17800.
27. Lorenz, M., Poole, K. J. V., Popp, D., Rosenbaum, G., and Holmes, K. (1995) *J. Mol. Biol. 246*, 108−119.
28. DasGupta, G., White, J., Phillips, M., Bulinski, J. C., and Reisler, E. (1990) *Biochemistry 29*, 3319−3324.

BI991873C